

## Structure of Au(110) Determined with Medium-Energy-Ion Scattering

M. Copel and T. Gustafsson

*Department of Physics, University of Pennsylvania, Philadelphia, Pennsylvania 19104*

(Received 19 March 1986)

Results of a study of the Au (110) reconstruction using medium-energy-ion scattering with channeling and blocking are reported. The data show clear and direct evidence for a missing-row model, unequivocally demonstrate that the first-layer spacing undergoes a large contraction, and show the presence of distortions in deeper layers. This model is similar to one derived from analysis of low-energy electron-diffraction data, but differs qualitatively with conclusions from x-ray scattering and transmission electron diffraction.

PACS numbers: 68.35.Bs, 61.16.Fk, 79.20.Nc

The (110) surfaces of the fcc metals consist of close-packed rows of atoms, separated by open space [Fig. 1(a)]. The open and anisotropic character of these surfaces has provided a number of instances of interesting structural behavior. It has, for example, been known for several years that the Au (110) surface, but not the isoelectronic Cu (110) and Ag (110), is reconstructed. Low-energy electron diffraction (LEED) shows a  $(1 \times 2)$  unit cell, indicating that alternate close-packed rows are inequivalent. While most investigations agree that a missing-row model is the most appropriate one,<sup>1-14</sup> there is substantial disagreement about the structure. From x-ray diffraction<sup>1</sup> and transmission electron microscopy<sup>2</sup> it has been claimed that there is a very significant outward relaxation of the spacing ( $d$ ) between the first two layers ( $\Delta d_{12} \approx +40\%$ ), while LEED<sup>3</sup> and low-energy-ion scattering<sup>4,5</sup> investigations obtain evidence for a large ( $\Delta d_{12} \approx -20\%$ ) inward relaxation. Helium-diffraction data also suggest a significant contraction.<sup>6</sup> High-energy-ion scattering experiments give evidence for substantial changes in  $d_{12}$  but fail to determine their sign.<sup>7-9</sup> Theoretical predictions have also spanned the range from contraction<sup>10,11</sup> to expansion.<sup>12,13</sup>

The structure of Au(110) is therefore quite controversial, with widely divergent competing models. The problem has a significant added dimension, because it is a system to which both traditional and emerging structural techniques have been applied. An assessment of the state of these emerging techniques<sup>1,2</sup> is therefore tied to the question of how well they describe the structure of Au(110). Au(110) is a good testing ground for comparative studies of structural techniques as samples can be prepared easily and reproducibly.

In this Letter we present results of a study of the Au (110) reconstruction using medium-energy-ion scattering (MEIS) with channeling and blocking.<sup>15</sup> Our results not only show distinct features associated with a missing-row structure, but also unequivocally demonstrate that  $d_{12}$  undergoes a large decrease. Our

data further show the presence of distortions in deeper layers, along the lines suggested in a structural model derived from LEED data.<sup>3</sup>

In MEIS, the angular distribution of the backscattered flux of particles that have undergone Rutherford scattering is measured with the incident beam aligned to a channeling direction of the target.<sup>15,16</sup> In a rigid lattice, only the first atom in a given row of atoms will be hit by an incoming ion; in a real crystal, vibrations will give rise to finite collision probabilities for the next few layers. The particles backscattered by the surface undergo fewer energy losses to electrons than

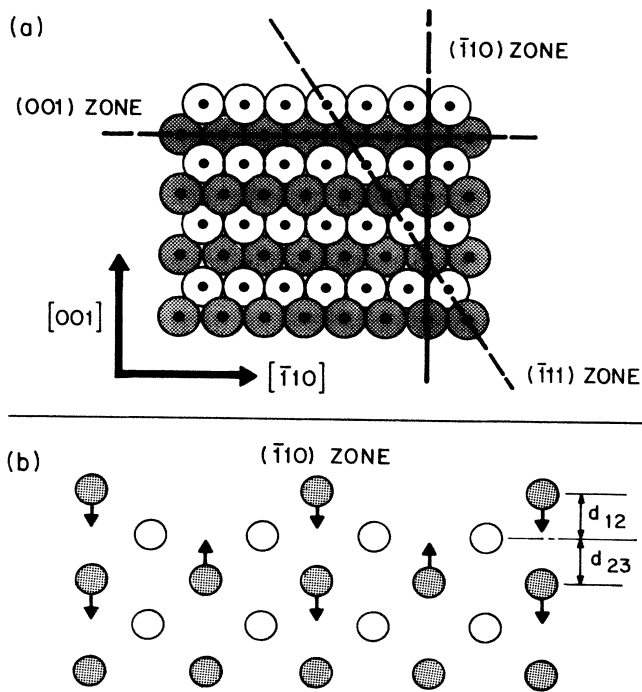


FIG. 1. (a) Top view of the Au (110) surface. The scattering planes in later figures are shown with dashed lines. (b) Side view. Arrows show the movements of the atoms in the model described in the text.

those that penetrate into the bulk and, therefore, the resulting energy distribution is dominated by a leading peak (the surface peak) composed of particles that have not penetrated into the bulk. MEIS uses both channeling and blocking; the angular distribution of the surface peak is measured with the incident beam in a channeling direction. These distributions are marked by blocking dips, where the surface atoms shadow particles backscattered from the lower layers. A change of interplanar separation at the surface shifts the position of the surface blocking dip away from the bulk crystallographic direction.<sup>15</sup>

A basic strength of MEIS is that qualitative information can be obtained by inspection of the direction of the shifts of blocking dips. By choice of different scattering geometries, it is possible to investigate each structural parameter separately, a distinct advantage over many other techniques. Below, we will first determine the superstructure, then measure the separation of the first two atomic layers, and finally investigate distortions in deeper layers.

MEIS is also a quantitative probe. Since the cross section for Rutherford scattering is well known, the scattering yields can be converted to an absolute number of atomic scatterers per unit area. The simple nature of the target-probe interaction allows simulation of the experiment by a Monte Carlo calculation, so that predictions based on specific structural models may be compared to experimental data.<sup>15, 16</sup>

The measurements were performed in an ultrahigh-vacuum chamber connected to a 200-keV proton accelerator.<sup>17</sup> Ion energies were measured with a toroidal electrostatic energy analyzer,<sup>18</sup> simultaneously measuring an angular range of 25°. The energy resolution was 700 eV at 100 keV and the angular uncertainty  $\pm 0.2^\circ$ . Three different samples were used in the present study, one of which had been the subject of earlier studies.<sup>4, 9</sup> All exhibited well-defined  $(1 \times 2)$  LEED patterns, very similar ion yields in double alignment, and angular shifts of blocking dips.

Our analysis below will be based on simple geometrical arguments, supported with simulations. We show first, on the basis of a qualitative argument, that there are major features in our spectra that determine the reconstruction model. In Fig. 2 we show data from the  $(\bar{1}10)$  zone with the ion beam incident in the  $[\bar{1}12]$  direction, which cuts directly across the rows of atoms that participate in the reconstruction (top panel). In the middle panel, we show the angular distribution of the surface peak intensity for Cu(110),<sup>19</sup> a surface that is not reconstructed. Strong, well-defined blocking dips are observed in the  $[114]$ ,  $[116]$ , and  $[118]$  directions, with the sizes of these dips falling off smoothly as higher index directions are reached. In the bottom panel, we show results for the reconstructed Au(110) surface. These results are dramatically

different from those of Cu(110) because of the pronounced attenuation of the  $[116]$  blocking dip. This can be understood quite easily from Fig. 2(a). In a missing-row model, the incident beam will penetrate unimpeded to the third atomic layer. In such a model, however, the first-layer atoms needed to block the backscattered flux are missing in the  $[116]$  direction and that blocking dip will vanish (the remnant of a dip in the spectra is due to deeper layers). These experimental results agree with a simulation of a crystal with a missing-row reconstruction [Fig. 2(c)]. We conclude, in agreement with earlier experimental studies,<sup>1-9, 14</sup> that the missing-row model is the correct one for the reconstruction of Au(110).

To analyze the structure in more detail, we need data in other scattering geometries. The  $(\bar{1}11)$  plane [Fig. 3(a)] provides a convenient geometry to measure the

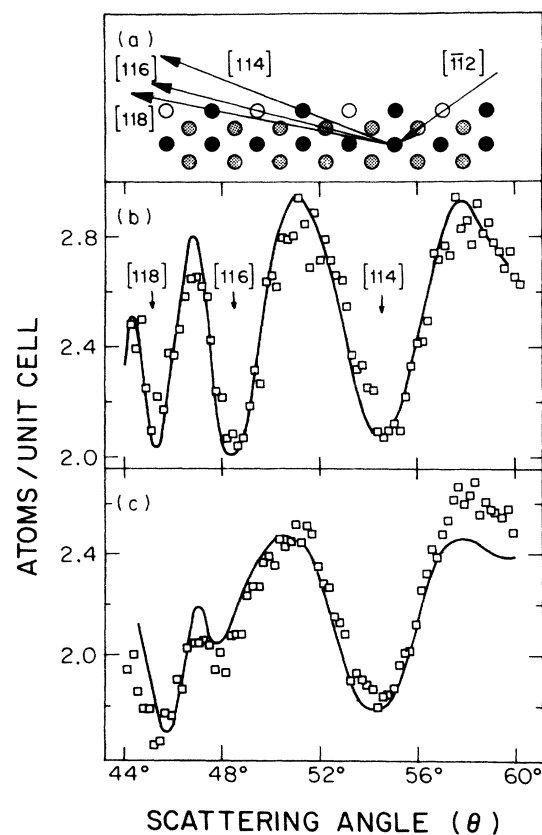


FIG. 2. (a) Side view of the  $(\bar{1}10)$  zone. This plane cuts perpendicularly across the rows in the surface, and includes the direction in which the surface unit cell is doubled. There is a second inequivalent scattering plane behind the plane, drawn in a lighter shading. Vacancies are shown as unfilled circles. (b) Angular distribution of the surface peak intensity in the  $(\bar{1}10)$  zone of Cu(110) for 100-keV protons incident in the  $[\bar{1}12]$  channeling direction. The blocking dips are in the  $[114]$ ,  $[116]$ , and  $[118]$  directions. The data have been normalized to the yield of a  $(1 \times 1)$  unit cell and the Rutherford cross section. (c) As (b) but for Au(110).

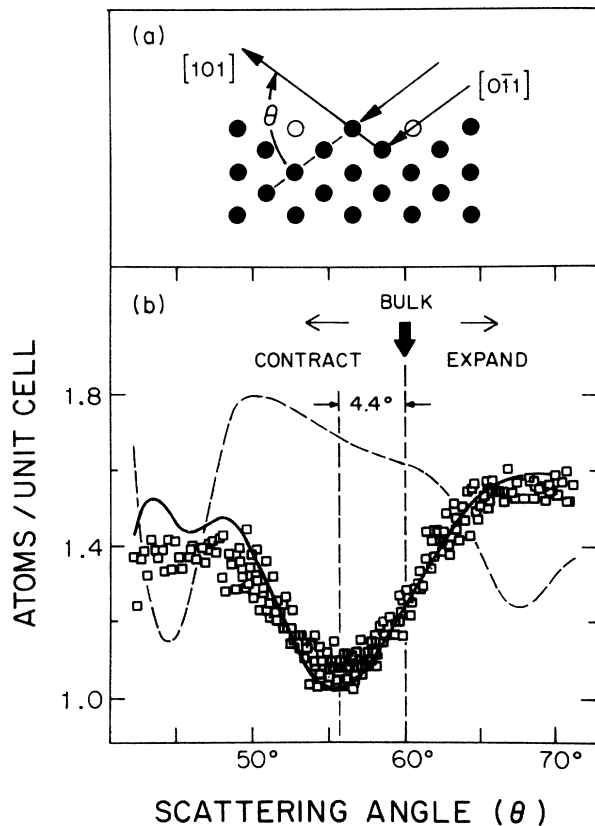


FIG. 3. (a) Side view of the  $(\bar{1}11)$  zone. This plane cuts diagonally across the rows in the surface, and includes all atoms in one single scattering plane. (b) Data taken in the  $(\bar{1}11)$  zone with 65-keV protons. The simulation for a 18% contracted surface is drawn with a solid line and for a surface with a 40% expansion is dashed. The bulk crystallographic direction is at  $60^\circ$ .

change in  $d_{12}$ . For our ion energies the backscattered flux will mainly contain contributions from the first two atomic layers. A shift of the blocking dip away from the ideal crystal value of  $60^\circ$  to smaller scattering angles corresponds to a contraction of  $d_{12}$ , while a shift to larger angles corresponds to an expansion. In Fig. 3(b) we show data collected with 65-keV protons incident in the  $[0\bar{1}1]$  channeling direction. The blocking-dip minimum is shifted  $4.4^\circ$  towards smaller scattering angles. This is the largest angular shift ever observed in channeling and blocking; the direction of the shift demonstrates a very substantial contraction of  $d_{12}$ . The yield in double alignment is slightly more than 1 atom/(unit cell), indicating that essentially all the scattering yield comes from the first two layers. A simulation with  $\Delta d_{12} = -18\%$  shows very good agreement with experiment (smooth line), while a simulation with  $\Delta d_{12} = +40\%$  (Refs. 1 and 2) has no obvious relation to the data (dashed line). The experiment was repeated at several incident ion energies and for both

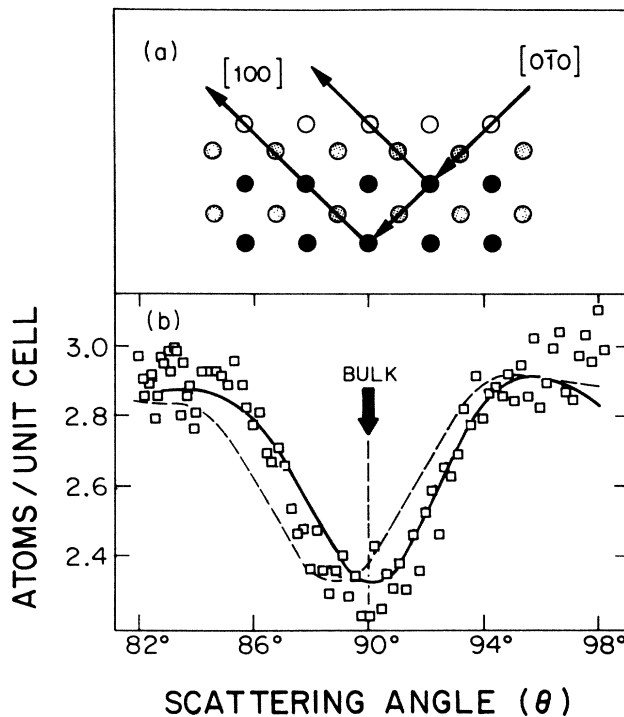


FIG. 4. (a) Side view of the  $(001)$  zone. This plane runs parallel to the rows in the surface. There are three inequivalent scattering planes, drawn with different shading. (b) Data taken in the  $(001)$  zone with 180-keV protons. The dashed line shows a simulation for a surface with a simple 18% contraction. The solid line is a simulation for a surface with an 18% contraction of  $d_{12}$ , a 4% expansion of  $d_{23}$ , and a buckling of the third layer (see text). The bulk blocking dip is at  $90^\circ$ .

normal ( $[110]$  channeling) and glancing ( $[0\bar{1}1]$  channeling) incidence with results consistent with those shown in Fig. 3(b).

The reconstruction must involve deeper layers also, as shown by data obtained in the  $(001)$  zone. In this geometry we sample a superposition of planes terminated by the first, second, and third atomic layers. This configuration is sensitive to distortions in the first three atomic layers [Fig. 4(a)]. Data from the  $[0\bar{1}0]$  channeling,  $[100]$  blocking configuration show [compared to those in Fig. 3(b)] at most a very slight angular shift from the bulk position of  $90^\circ$  [Fig. 4(b)]. Since, as shown earlier,  $d_{12}$  is contracted, there must be distortions in deeper layers that compensate the shift caused by the first-layer contraction. In order to quantify this conclusion, we have performed extensive simulations and an  $R$ -factor analysis. On the basis of these simulations, we believe that the most significant structural change after the first-layer contraction is a buckling in the third layer. The effect of buckling was quite small in the  $(\bar{1}11)$  zone (Fig. 3), but simulations for the  $(001)$  zone (Fig. 4) were strongly influenced.

Significant ( $> 0.1 \text{ \AA}$ ) pairing in the second layer resulted in absolute yields that were larger than the experimentally measured ones. Simple triangulation may be used to demonstrate that pairing only weakly affects the angular shift in the  $(\bar{1}11)$  zone. The details of this analysis will be presented elsewhere; as an example we show in Fig. 4(b) the simulated results obtained with only a  $-18\%$  contraction (clearly inadequate) and with the model we favor, which also involves an expansion of  $d_{23}$  by  $4\%$  and buckling of the third layer by  $14\%$  ( $0.2 \text{ \AA}$ ). In the buckling mode, the atom directly under the first-layer atom moves toward the bulk by  $7\%$  of an interplanar spacing, and the inequivalent third-layer atom moves out  $7\%$  [see Fig. 1(b)]. As in other ion-scattering simulations,<sup>15,16,19</sup> we use a surface Debye temperature ( $130 \text{ K}$ ) exponentially decaying to the bulk value of  $170 \text{ K}$ , with a nearest-neighbor correlation of  $0.3$ , which we judge to be equivalent to the correlations in Ref. 9. This model is similar to the one proposed by Moritz and Wolf on the basis of a LEED analysis,<sup>3</sup> the most notable difference being that we place less emphasis on pairing in the second layer. It is difficult to differentiate clearly between second-layer pairing and the influence of vibrations; nevertheless, our data may be adequately modeled without pairings as large as the x-ray result.<sup>1</sup>

Our results are more detailed than those from low-energy-ion scattering<sup>4,5</sup> and He diffraction,<sup>6</sup> but the magnitude and sign of  $\Delta d_{12}$  are in reasonable agreement. While high-energy-ion scattering only determined bounds on  $\Delta d_{12}$  and not the direction of the relaxation,<sup>8,9</sup> those bounds are compatible with our findings. We have no simple explanation for the significant differences between the present results and those from x-ray diffraction<sup>1</sup> and electron microscopy.<sup>2</sup>

We thank P. O. Nilsson, D. Zehner, and W. R. Graham for supplying the crystals. This research was supported by the National Science Foundation under

Grants No. DMR 80-15302, No. 82-16718, and No. 83-09652.

- 
- <sup>1</sup>I. K. Robinson, Phys. Rev. Lett. **50**, 1145 (1983).  
<sup>2</sup>L. D. Marks, Phys. Rev. Lett. **51**, 1000 (1983).  
<sup>3</sup>W. Moritz and D. Wolf, Surf. Sci. **163**, L655 (1985).  
<sup>4</sup>S. H. Overbury, W. Heiland, D. M. Zehner, S. Datz, and R. S. Thoe, Surf. Sci. **109**, 239 (1981).  
<sup>5</sup>H. Hemme and W. Heiland, Nucl. Instrum. Methods Phys. Res. Sect. B **9**, 41 (1985). See also J. Möller, H. Niehus, and W. Heiland, Surf. Sci. **166**, L111, (1986).  
<sup>6</sup>M. Manninen, J. K. Nørskov, and C. Umrigar, Surf. Sci. **88**, L393 (1982).  
<sup>7</sup>D. P. Jackson, T. E. Jackman, J. A. Davies, W. A. Unertl, and P. D. Norton, Surf. Sci. **126**, 226 (1983).  
<sup>8</sup>I. K. Robinson, Y. Kulk, and L. C. Feldman, Phys. Rev. B **29**, 4762 (1984).  
<sup>9</sup>S. P. Withrow, J. H. Barrett, and R. J. Culbertson, Surf. Sci. **161**, 584 (1985).  
<sup>10</sup>H.-J. Brocksch and K. H. Bennemann, Surf. Sci. **161**, 321 (1985).  
<sup>11</sup>T. Halicioğlu, T. Takai, and W. A. Tiller, in *The Structure of Surfaces*, edited by M. A. van Hove and S. Y. Tong, Springer Series in Surface Sciences Vol. 2 (Springer, Berlin, 1985), p. 231.  
<sup>12</sup>H.-J. Brocksch and K. H. Bennemann, in Ref. 11, p. 226.  
<sup>13</sup>V. Heine and L. D. Marks, Surf. Sci. **165**, 65 (1986).  
<sup>14</sup>G. Binnig, H. Rohrer, Ch. Gerber, and E. Weibel, Surf. Sci. **131**, L379 (1983).  
<sup>15</sup>J. F. van der Veen, Surf. Sci. Rep. **5**, 199 (1985).  
<sup>16</sup>L. C. Feldman, J. W. Mayer, and S. T. Picraux, *Materials Analysis by Ion Channeling* (Academic, New York, 1982).  
<sup>17</sup>W. R. Graham, S. M. Yalisove, E. D. Adams, T. Gustafsson, M. Copel, and E. Törnqvist, to be published.  
<sup>18</sup>R. G. Smeenk, R. M. Tromp, H. H. Kersten, A. J. H. Boerboom, and F. W. Saris, Nucl. Instrum. Methods Phys. Res. **195**, 581 (1982).  
<sup>19</sup>M. Copel, T. Gustafsson, W. R. Graham, and S. M. Yalisove, Phys. Rev. B **33**, 8110 (1986).

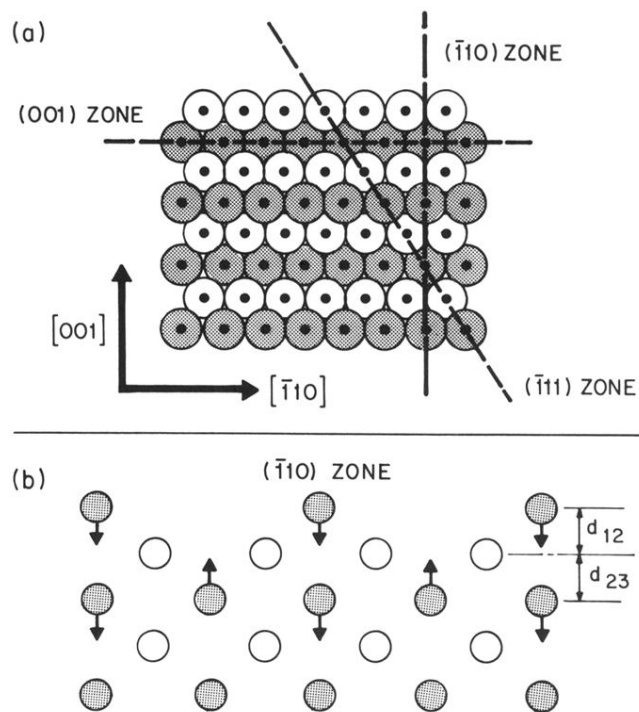


FIG. 1. (a) Top view of the Au (110) surface. The scattering planes in later figures are shown with dashed lines. (b) Side view. Arrows show the movements of the atoms in the model described in the text.

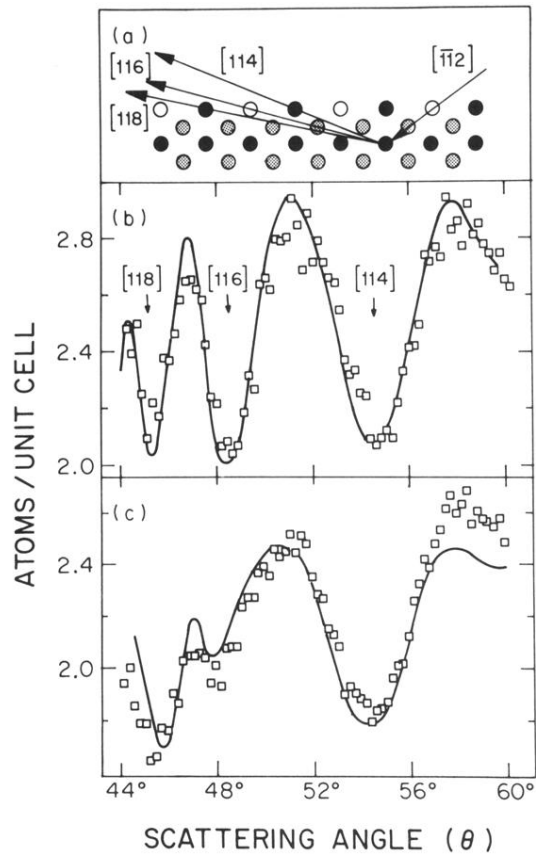


FIG. 2. (a) Side view of the  $(\bar{1}10)$  zone. This plane cuts perpendicularly across the rows in the surface, and includes the direction in which the surface unit cell is doubled. There is a second inequivalent scattering plane behind the plane, drawn in a lighter shading. Vacancies are shown as unfilled circles. (b) Angular distribution of the surface peak in the  $(\bar{1}10)$  zone of Cu(110) for 100-keV protons incident in the  $[\bar{1}\bar{1}2]$  channeling direction. The blocking dips are in the  $[114]$ ,  $[116]$ , and  $[118]$  directions. The data have been normalized to the yield of a  $(1 \times 1)$  unit cell and the Rutherford cross section. (c) As (b) but for Au(110).

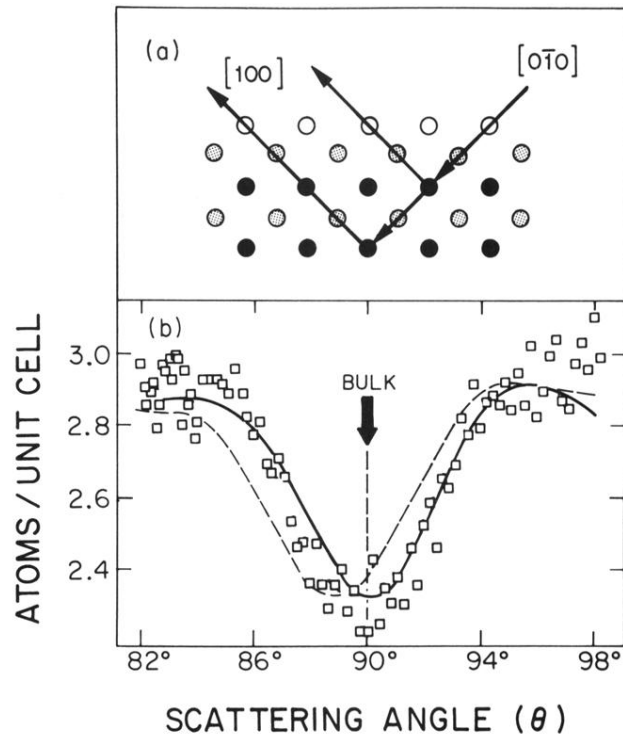


FIG. 4. (a) Side view of the (001) zone. This plane runs parallel to the rows in the surface. There are three inequivalent scattering planes, drawn with different shading. (b) Data taken in the (001) zone with 180-keV protons. The dashed line shows a simulation for a surface with a simple 18% contraction. The solid line is a simulation for a surface with an 18% contraction of  $d_{12}$ , a 4% expansion of  $d_{23}$ , and a buckling of the third layer (see text). The bulk blocking dip is at  $90^\circ$ .